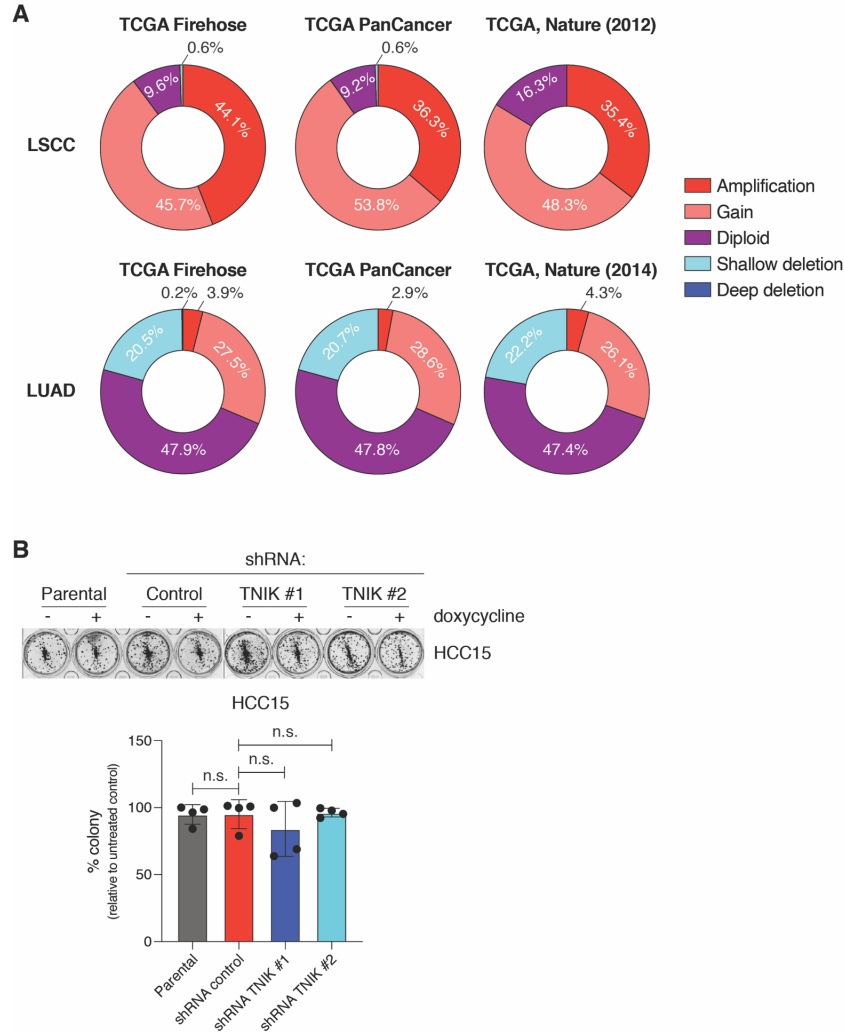
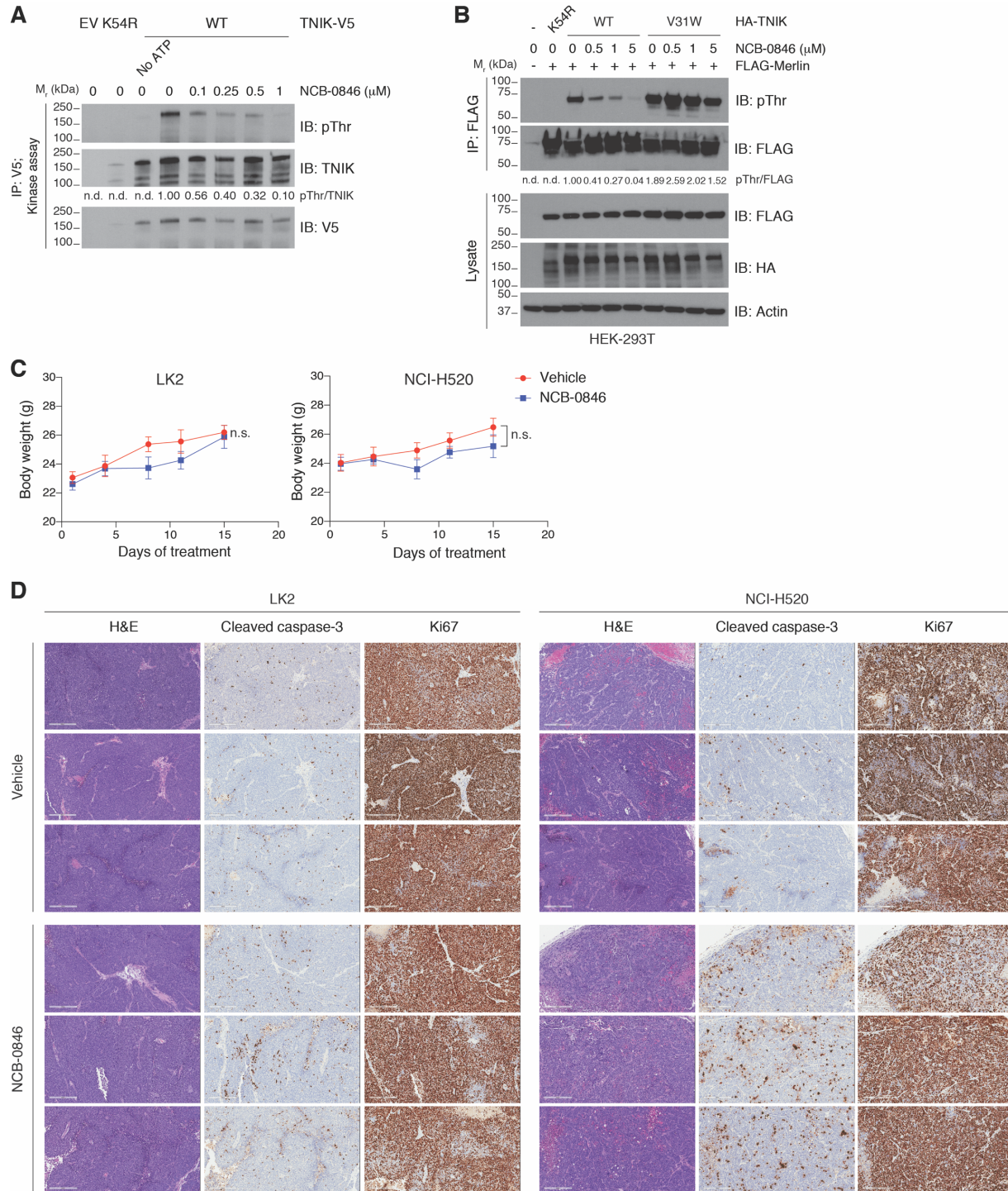


Supplementary Figures

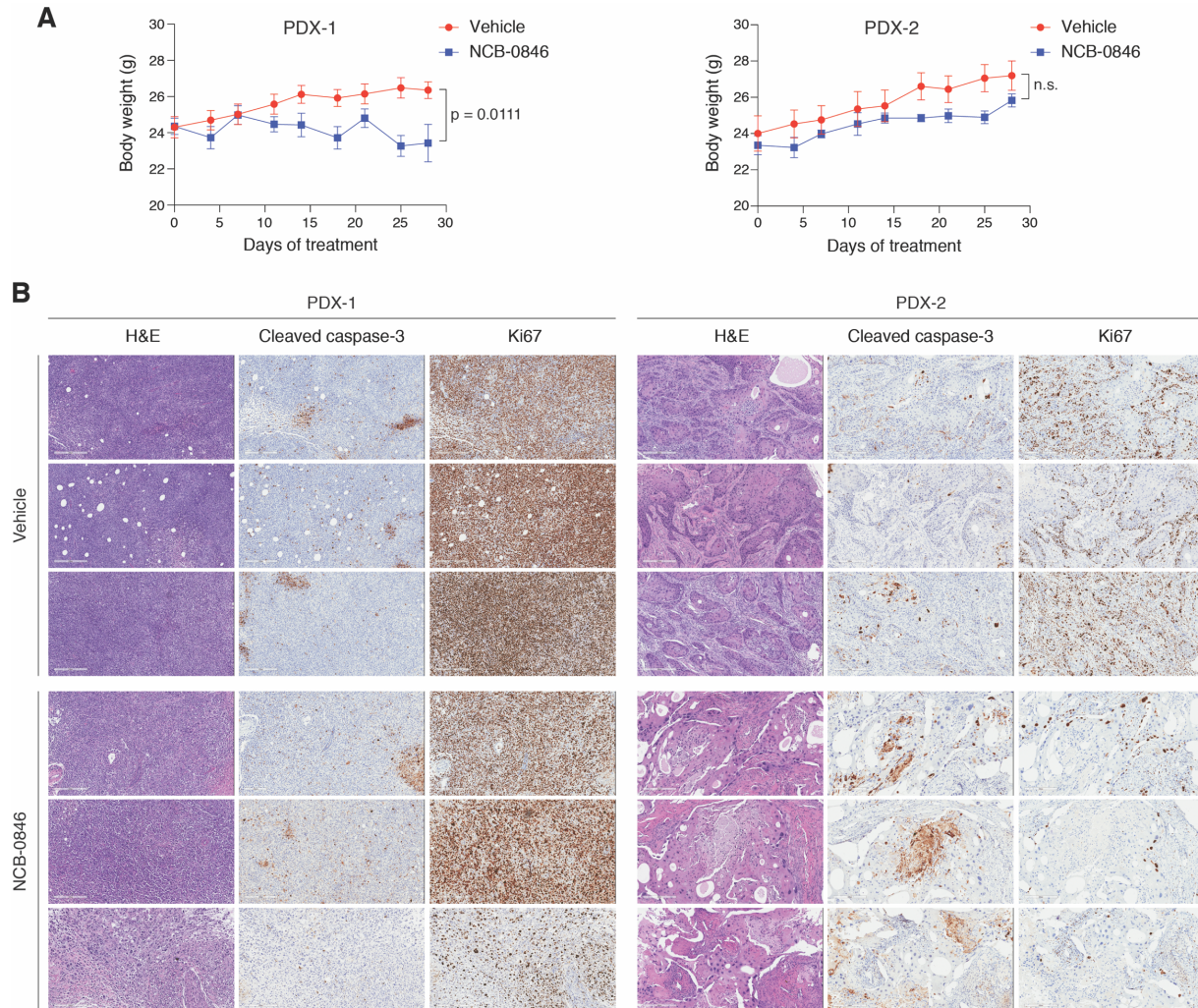


Supplementary Figure S1. A. Distribution of *TNIK* genomic alterations in lung squamous cell carcinoma (LSCC) and lung adenocarcinoma (LUAD) from different TCGA datasets. The data were extracted from cBioPortal (1) and the graph generated with Prism 8. **B.** Colony formation assay (14 days) of HCC15 cells following dox-inducible (1 $\mu\text{g}/\text{ml}$, replaced every 48 h) *TNIK* knockdown. The image is representative of four independent experiments. Data are represented as mean value \pm SD, one-way ANOVA, Tukey's multiple comparisons post-test. n.s., not significant.

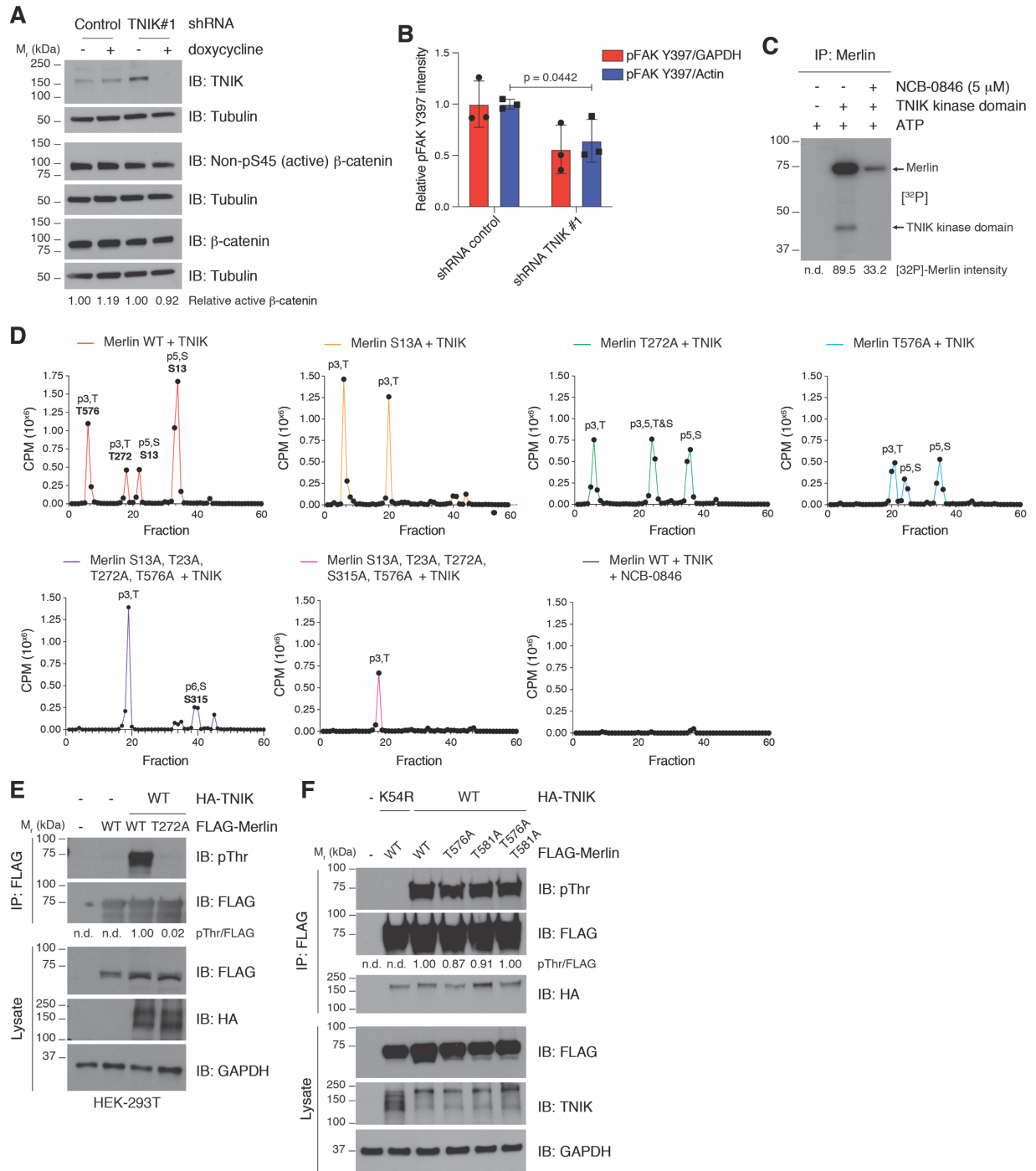


Supplementary Figure S2. A. *In vitro* kinase assay of immunoprecipitated TNIK with different doses of NCB-0846. TNIK autophosphorylation was assessed with a pan-phospho-threonine antibody, and normalized to TNIK levels in the immunoprecipitates. Band intensity was quantified with ImageJ ($n = 3$ independent experiments). **B.** Generation and characterization of a TNIK

inhibitor-resistant mutant (TNIK V31W). TNIK and Merlin were co-expressed in HEK-293T (16 h), after which cells were treated at the indicated NCB-0846 concentrations (1 h). FLAG-Merlin was immunoprecipitated and phosphorylation assessed with a pan-phospho-threonine antibody. Band intensity was quantified with Image J (n = 3 independent experiments). **C.** Mouse body weight curve of LK2-cell-derived xenografts (left, n = 10 mice in the vehicle-treated group; 8 mice in the NCB-0846-treated group.) and NCI-H520-cell-derived xenografts (right, n = 10 mice in the vehicle-treated group; 9 mice in the NCB-0846-treated group) treated with NCB-0846 (100 mg/kg, b.i.d., five days on/two days off). Mean mouse body weight \pm SEM are shown; two-tailed t-test (LK2); two-tailed Mann–Whitney test (NCI-H520). n.s., not significant. **D.** Representative hematoxylin and eosin (H&E), cleaved caspase-3 and Ki67 immunohistochemistry images from LK2- (left) and NCI-H520 (right) cell derived tumors treated with vehicle or NCB-0846. Scale bar = 300 μ m.

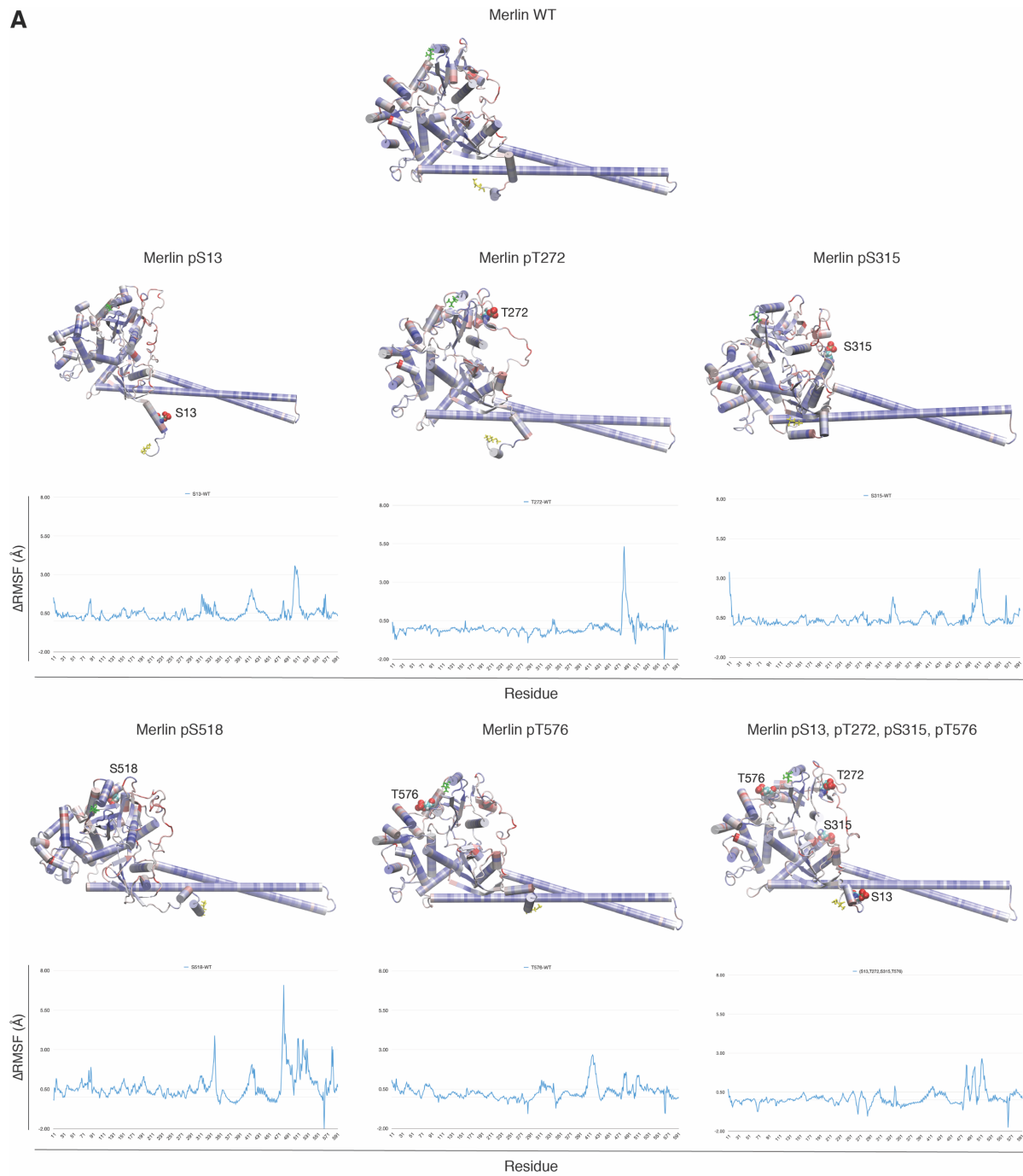


Supplementary Figure S3. A. Mouse body weight curve of PDX-1 (left, $n = 8$ mice/group) and PDX-2 (right, $n = 9$ mice/group) LSCC-derived patient xenografts treated with NCB-0846 (100 mg/kg, b.i.d., five days on/two days off). Mean mouse weight \pm SEM are shown; two-tailed t-test with Welch's correction (PDX-1); two-tailed t-test (PDX-2). n.s., not significant. **B.** Representative hematoxylin and eosin (H&E), cleaved caspase-3 and Ki67 immunohistochemistry images from PDX-1 (left) and PDX-2 (right) models treated with vehicle or NCB-0846. Scale bar = 300 μ m.

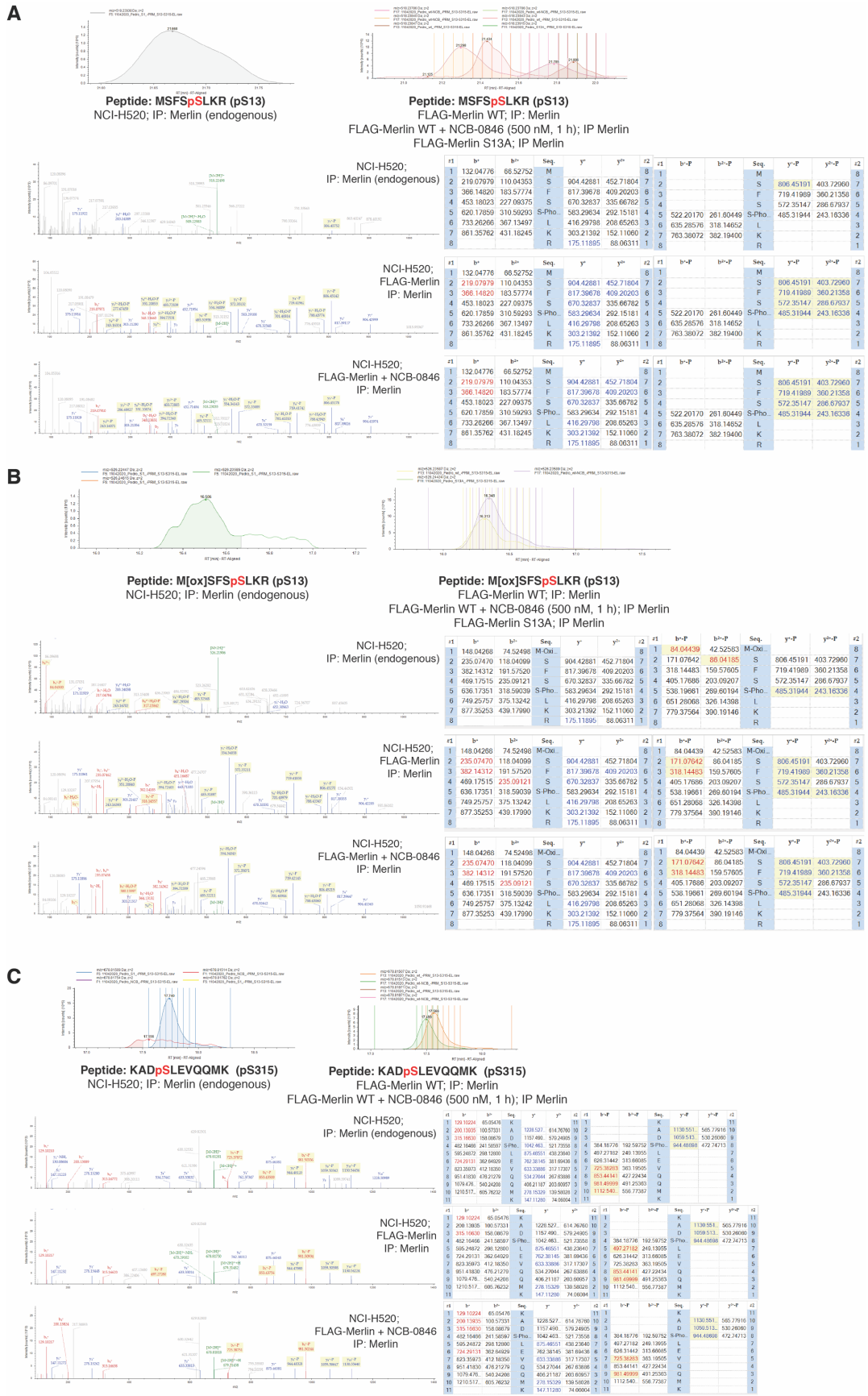


Supplementary Figure S4. A. Analysis of β-catenin levels and activation in LK2 cells after dox-induced (1 μg/ml, 72 h) TNIK knockdown. **B.** Reverse phase protein array analysis of TNIK knockdown in LK2 cells leads to the downmodulation of FAK Y397 phosphorylation. **C.** Radioactive (γ[³²P]-ATP) in vitro kinase assay of immunoprecipitated Merlin in the presence or absence of purified TNIK-kinase domain (50 ng) and NCB-0846 (5 μM), used for peptide

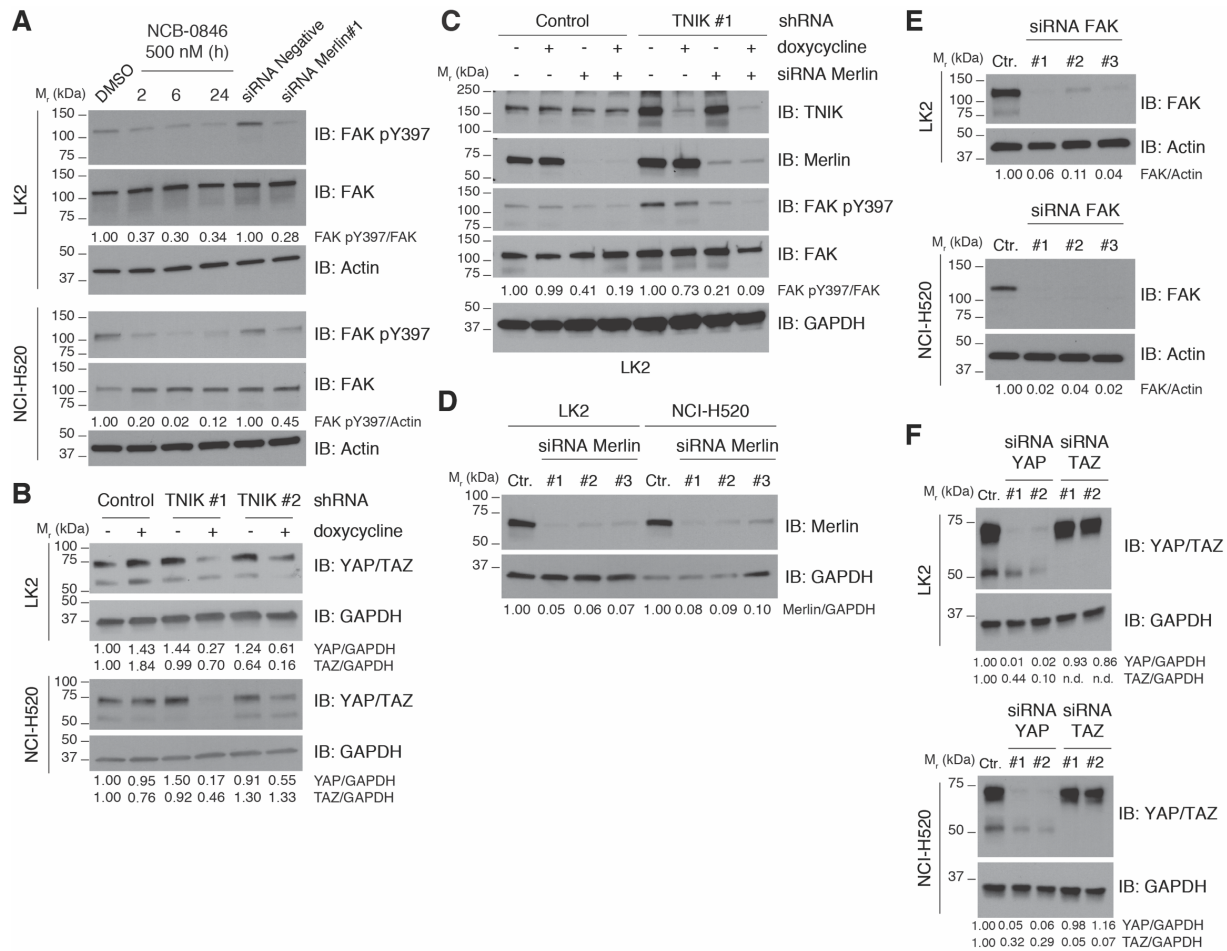
mapping. The assay is representative of three independent experiments. **D.** Chromatograms of γ [³²P]-labelled Merlin mutants following in vitro kinase assays to identify TNIK-mediated phosphorylation sites by peptide mapping. Corresponding phosphorylation sites are specified for each peak. **E.** Validation of Merlin pT272 by co-expression of TNIK and Merlin wild-type (WT) or the non-phosphorylatable mutant T272A in HEK 293T cells from two independent experiments. **F.** Analysis of Merlin pT576 and pT581 by co-expression of TNIK and Merlin wild-type (WT) or the non-phosphorylatable mutants T576A, T581A and the double mutant in HEK 293T cells from two independent experiments. n.d.: not detected. Tubulin or GAPDH were used as loading controls. Band intensity was quantified using ImageJ.

A

Supplementary Figure S5. Structural modeling and molecular dynamics simulations of Merlin phosphorylated at S518 (PKA, PAK2 site) and TNIK-identified phosphosites (S13, T272, S315, and T576).



Supplementary Figure S6. A-C. Mass spectrometry analysis of phosphopeptides corresponding to Merlin phospho-serine 13 (pS13, A and B) and phospho-serine 315 (pS315, C) from endogenous and overexpressed Merlin pulldowns in NCI-H520 cells. No detectable peaks for pS13 were observed in the endogenous Merlin pulldown from NCB-0846-treated cells (500 nM, 1 h), nor in the FLAG-Merlin S13A condition.



Supplementary Figure S7. A. Reduced activation of FAK (measured as FAK pY397) after treatment with NCB-0846 (500 nM) for the indicated times or Merlin knockdown (72 h) in LK2 and NCI-H520 cells. **B.** Dox-inducible (1 μ g/ml, 72 h) knockdown of TNIK reduces YAP levels in LK2 and NCI-H520 cells. The data are representative of three independent experiments. **C.** Combined knockdown of Merlin (96 h) and TNIK (with doxycycline 1 μ g/ml, 72 h) results in FAK inhibition in LK2 cells (n = 3 independent experiments). **D-F.** Control of efficient Merlin (D), FAK (E) and YAP/TAZ (F) siRNA-mediated knockdown (96 h) in LK2 and NCI-H520 cells (related to Fig. 4I, 4J). The data are representative of n \geq 3 independent experiments. n.d.: not detected. GAPDH or Actin were used as loading controls. Band intensity was quantified using ImageJ.

Supplementary References

1. Cerami E, Gao J, Dogrusoz U, Gross BE, Sumer SO, Aksoy BA, *et al.* The cBio cancer genomics portal: an open platform for exploring multidimensional cancer genomics data. *Cancer Discov* **2012**;2(5):401-4 doi 10.1158/2159-8290.CD-12-0095.